A Robust Extraction Approach of Auditory Brainstem Response Using Adaptive Kalman Filtering Method

Haoshi Zhang, Mingxing Zhu, Yanbing Jiang, Dan Wang, Xin Wang, *Student Member, IEEE*, Zijian Yang, Weimin Huang, Shixiong Chen, *Member, IEEE*, and Guanglin Li, *Senior Member, IEEE*

***Abstract*—*Objective:* The Auditory brainstem response (ABR) can provide valuable information on the function of the auditory pathway. However, the ABR signal has a very small amplitude, and it is easily submerged in different background noises with large amplitude. Conventional ABR extraction methods such as time-domain averaging (TDA) and Kalman filter (KF) were greatly affected by noise intensity, and the result relies on the empirical settings of parameters. ABR extraction method that can automatically adjust parameters to adapt different background noises was needed. *Methods:* An adaptive Kalman filtering (AKF) based ABR signal extraction method was proposed, in which two recursive rules were introduced to constantly update the parameters according to the real-time noise properties. It was used for ABR extraction from recordings in noises with different orders of larger magnitude. *Results:* The AKF method demonstrated the best performance in obtaining reliable ABR waveform morphologies in the presence of large EMG noises compared with traditional methods of TDA or KF. It could extract satisfactory ABR signal with fewer trials of acoustic stimulus repetition, even from noise 10000 times larger than ABR signal. The AKF results also showed smaller absolute errors and higher correlation coefficients with the target ABR signal when different types (gum chewing, mouth opening and milk drinking) or levels of noises were introduced. *Conclusion:* The proposed AKF method is a great candidate to increase the robustness of current ABR measurements. *Significance:* It could provide reduced testing time and relaxed recording conditions for ABR and other evoked potentials extraction.**

***Index Terms*—Auditory brainstem response (ABR), adaptive Kalman filter (AKF), background noise (BN).**

Manuscript received 22 September 2021; revised 17 April 2022; accepted 20 May 2022. Date of publication 27 May 2022; date of current version 22 November 2022. This work was supported in part by the National Natural Science Foundation of China under Grants 61901464, 81927804, and 62101538, in part by Shenzhen Governmental Basic Research under Grant JCYJ20180507182241622, in part by the Science and Technology Planning Project of Shenzhen under Grants JSGG20210713091808027 and JSGG20211029095801002, in part by the Shandong Institute of Advanced Technology, Chinese Academy of Sciences under Grant YJZX003, and in part by the SIAT Innovation Program for Excellent Young Researchers under Grant E1G027. *(Haoshi Zhang and Mingxing Zhu contributed equally to this work.) (Corresponding authors: Shixiong Chen; Guanglin Li.)*

Haoshi Zhang, Yanbing Jiang, and Xin Wang are with the CAS Key Laboratory of Human-Machine Intelligence-Synergy Systems, Shenzhen Institutes of Advanced Technology, Chinese Academy of Sciences and the Shenzhen College of Advanced Technology, University of Chinese Academy of Sciences, China.

Mingxing Zhu is with the School of Electronics and Information Engineering, Harbin Institute of Technology, Shenzhen and the CAS Key Laboratory of Human-Machine Intelligence-Synergy Systems, Shenzhen Institutes of Advanced Technology, Chinese Academy of Sciences, China.

Dan Wang and Zijian Yang are with the CAS Key Laboratory of Human-Machine Intelligence-Synergy Systems, Shenzhen Institutes of Advanced Technology, Chinese Academy of Sciences, China, and also with the Guangdong-Hong Kong-Macao Joint Laboratory of Human-Machine Intelligence-Synergy Systems, China.

Weimin Huang is with the Department of Neonatology, Shenzhen Children's Hospital, China.

Shixiong Chen and Guanglin Li are with the CAS Key Laboratory of Human-Machine Intelligence-Synergy Systems, Shenzhen Institutes of Advanced Technology, Chinese Academy of Sciences, Shenzhen 518055, China and also with the Guangdong-Hong Kong-Macao Joint Laboratory of Human-Machine Intelligence-Synergy Systems, Shenzhen 518055, China (e-mail: sx.chen@siat.ac.cn; gl.li@siat.ac.cn).

Digital Object Identifier 10.1109/TBME.2022.3178550

I. Introduction

THE auditory brainstem response (ABR), also known as brainstem auditory Evoked Potentials (BAEP), is a sound-evoked neural response of the auditory pathway recorded from electrodes placed on the scalp [1]. It consists of up to 7 positive wave peaks (labeled as I-VII) and can provide valuable information on the function of different relay stations along the ascending auditory pathway [2]. The abnormal changes of latency and amplitude of the ABR wave peaks might reflect possible neurological abnormalities such as auditory neuropathy, Gaucher disease, and vestibular schwannomas [3]. Moreover, the ABR measurement is totally objective without the need for subjects' responses, and it can be measured even when the subject is sleeping. Therefore, it is widely used in hearing screening of newborns and objective estimation of hearing thresholds of young children or adults who cannot perform behavioral audiogram tests [4]–[7].

As one kind of evoked potentials, ABR signal has very small amplitude, with only 0.1–1 μV in normal-hearing subjects, and it is easily submerged in other background noises with much larger amplitude, such as the electrocardiogram (ECG), electromyography (EMG) and spontaneous electroencephalogram (EEG) signals [2]. The characteristics of ultra-low amplitude make the ABR measurement rather challenging, and therefore different approaches have been proposed to extract the small ABR signal from the recordings inevitably contaminated by various noises. Time-domain averaging (TDA) is one of the

techniques commonly used in the ABR signal extraction in both clinic and research scenarios. By averaging a set of replicate trials in the time domain, the method of TDA can increase the signal-to-noise ratio (SNR) by a factor in proportion to the square root of the repeated trial number when the noise is random and stationary [8]–[11], suggesting that the SNR can keep improved as long as the trial number is increasing. While in clinical practices, it is usually rather difficult for infants and young children to keep a stationary state for a long time, leading to the necessity of mild sedation for them to stay quiet [12]–[14]. Moreover, noises introduced by EMG signals, powerline interferences, and electrode movements can not be avoided and would be recorded inevitably in most situations. The low-amplitude nature and introduction of various noises make it compulsory to repeat the stimulation for a large number of trials to achieve satisfactory measurement results, resulting in a too long time in ABR measurement that is unacceptable in clinical applications. Therefore, there is an urgent need for advanced signal processing technology to reduce the impact of strong noise interference during the ABR signal extraction.

Various signal processing techniques have been employed to minimize the residual noise in the recorded ABR signal, including wavelet transform, signal filtering, artifact rejection, and weighted average [14]–[20]. Wavelet transform was used in tracking temporal variations of the ABR measurements, nevertheless it required the establishment of threshold functions and time window as an integral part [15]. The computation complexity also makes the wavelet method not applicable in real-time circumstances. Artifact rejection and weighted average techniques attracted the most attention in clinical applications and previous studies. The artifact rejection method improves the SNR by excluding those segments wherein the noise level is higher than the preset criterion [11], [17]. The criterion could be a fixed amplitude level or a percentage level of the averaged response amplitude. However, the choice of the preset criterion is quite arbitrary and largely dependent on the experience of the experimenter. Additionally, the noise level could change in amplitude over time, making the fixed criterion method problematic in many cases. The method of weighted average allows all segments into the average and assigns each segment with a weight coefficient in inverse proportion to its estimated noise level, resulting in larger weights for segments with higher SNRs [9], [18]–[20]. However, the accurate estimate of the noise level is rather challenging, providing that both the signal and noises remain unknown [21]–[23].

Additionally, as one kind of linear optimal filter, Kalman filter (KF) has been widely used due to its great performance, relatively simple form, and small computational power. Many previous studies have demonstrated the superior performance of the KF method in the application of signal state extimation and evoked potential extraction [24], [25]. Nevertheless, the conventional KF algorithm relies heavily on the assumption of the system model and the prior knowledge of the noise characteristics. In practical applications, users usually have to manually guess the covariance of the process noise (Q) and covariance matrix of the measurement noise (R), according to their prior knowledge of the signals. However, it is rather difficult to set the optimal values of the parameters manually and inappropriate parameter guess would lead to the failure of achieving desired filter outcomes or even divergence of the output [26]–[28]. Moreover, the statistical characteristics of noise may change with time for actual systems, causing the conventional method with a fixed parameter setting to be problematic in real application scenarios. With the development of signal processing theories, adaptive Kalman filter (AKF) technology was proposed to reduce or bound the noise errors by modifying or adapting the algorithm to the dynamic change of the real data. A number of approaches have been taken to estimate the unknown priori statistics of noise from the observed data [29]–[36]. The multiple model Bayesian approach estimated the state and measurement noises by computing the Bayesian probability of a bank of different models [34]. The maximum likelihood method imporoved the adaptivity of the Kalman filter by maximizing the likelihood function of the innovations to estimate the covariances [35]. However, both the Bayesian and maximum likelihood methods are based on the assumption that the dynamic error is time-invariant and the implementations are computationally expensive. The correlation technique estimates the covariance matrices based on the sample autocorrelations of the innovations [36]. Nevertheless, large windows of data samples are required by the correlation technique to achieve reliable estimate of the noise covariance parameters, making it not applicable for scenarios with rapidly varying noises.

In this study, a new AKF-based method was proposed to extract the target ABR signals from recordings with different noises, in which, two recursive updating rules based on covariance matching principle were introduced to constantly update the state noise covariance matrix Q and the measured noise covariance matrix R according to the real-time noise properties. The performance of the proposed method was examined by comparing the absolute error (AE) and correlation coefficient (CC) of the ABR signals extracted by different algorithms. The time reduction of achieving satisfactory ABR waveforms and the robustness of the AKF method under different noise conditions were also investigated. The proposed AKF method of this study may help to improve the signal quality of the ABR measurements in different recording situations and therefore increase the accuracy of the diagnoses of different neurological abnormalities of the auditory system.

II. Method

A. AKF-Based ABR Signal Extraction

The algorithm of the proposed AKF method for ABR signal extraction was extended from the traditional KF, whose system model could be represented by the following (1) and (2):

$$x_k = Ax_{k-1} + w_{k-1} \tag{1}$$

$$z_k = Hx_k + v_k \tag{2}$$

In (1), x_{k-1} and x_k represent the n-dimensional (n-point) true states in response to the (k-1)th and k^{th} trials of the click stimulus, respectively; the matrix A is the state transition model applied to the previous state x_{k-1}, and w_{k-1} is the process noise. In (2),

the k^{th} measurement z_k could be modeled by mapping the true state x_k into the observed space using the observation model H, plus the measurement noise v_k. Physiologically, the ABR signal evoked by the repetitive trials of the same click stimulus should be nearly identical. Therefore, both the matrix A and H were set as identity matrix in above model. The process noise w_k and measurement noise v_k are both assumed to be Gaussian white noises, and their covariances (labeled as Q_k and R_k, respectively) could be calculated as:

$$E\left\{w_k w_k^T\right\} = Q_k \tag{3}$$

$$E\left\{v_k v_k^T\right\} = R_k \tag{4}$$

The recursive process of the proposed AKF method is similar to that of the traditional KF (except the updating rules of Q_k and R_k) and is divided into two steps: prediction and correction. During the prediction step, we first obtain the current predicted ABR vector $\bar{x}_k$ from the prior estimated ABR vector $\hat{x}_{k-1}$ according to (5), and then predict state error covariance matrix $\bar{P}_k$ from prior state error covariance matrix $\hat{P}_{k-1}$ and state noise covariance matrix Q_{k-1} (6):

$$\bar{x}_k = A\hat{x}_{k-1} \tag{5}$$

$$\bar{P}_k = A\hat{P}_{k-1}A^T + Q_{k-1} \tag{6}$$

During the correction step, the innovation or measurement pre-fit residual $\bar{e}_k$ is calculated from the difference between the current k^{th} ABR measurement z_k and the current predicted ABR vector $\bar{x}_k$ (7). Then the Kalman gain K_k, which defines the updating weight of the innovation during the correction step, is computed from the predicted state error covariance matrix $\bar{P}_k$ and the measurement noise covariance matrix R_k (9). Thereafter, they are used to correct the predicted current ABR vector $\hat{x}_k$ and state error covariance matrix $\hat{P}_k$ from the previous prediction steps as follows:

$$\bar{e}_k = z_k - H\bar{x}_k \tag{7}$$

$$\hat{e}_k = \frac{N-1}{N}\hat{e}_{k-1} + \frac{1}{N}\bar{e}_k \tag{8}$$

$$K_k = \bar{P}_k H^T \left(H\bar{P}_k H^T + R_k\right)^{-1} \tag{9}$$

$$\hat{x}_k = \bar{x}_k + K_k\hat{e}_k \tag{10}$$

$$\hat{P}_k = \left(I - K_k H\right)\bar{P}_k \tag{11}$$

For the proposed AKF method, the major deviation from the traditional KF is to dynamically update the Q_k and R_k parameters so that they can keep track of the instantaneous change of noises. In this study, two recursive updating rules based on covariance matching principles are introduced for the adaptive estimation of the filter parameters [27], [31], [32]. For a given integer parameter N, the increment of state noise covariance matrix ΔR_k is estimated by the innovation $\bar{e}_k$ according to (12), and then the current R_k parameter is updated according to ΔR_k:

$$\Delta R_k = \frac{1}{N-1}\left(\hat{e}_k - \bar{e}_k\right)\left(\hat{e}_k - \bar{e}_k\right)^T - \frac{1}{N}\left(H\bar{P}_k H^T\right) \tag{12}$$

$$R_k = \left|diag\left(\frac{N-1}{N}R_{k-1} + \Delta R_k\right)\right| \tag{13}$$

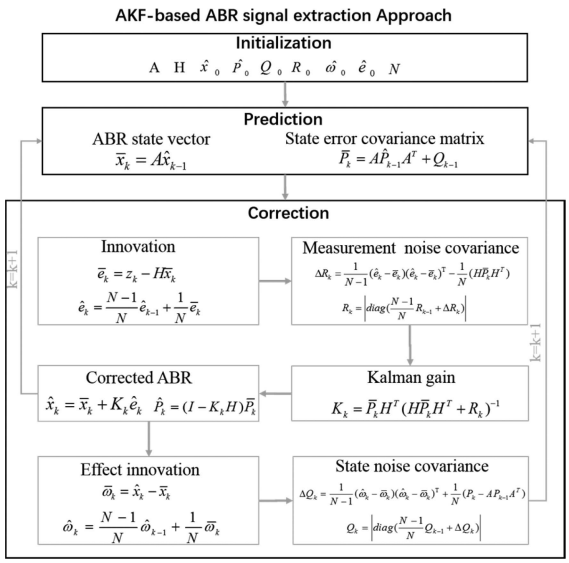

Fig. 1. Implementation flowchart of the proposed AKF-based method for ABR signal extraction.

In the above equations, the parameter N of the AKF method is an adjustable scale factor, and its value determines the contribution weight relationship between the previous and the current increment value to the Kalman gain. A larger N parameter indicates that more weight is applied to the previous estimate value, and less weight is given to the current data in the noise covariance matric estimation process. The parameter N actually adjusts the adaptation speed of Q_k and R_k parameters of the AKF filter to match the new noise conditions. Smaller N values lead to faster adaptation speeds, but oscillations in the adaption will happen if the N value is too small. In the process of suppressing the stationary random system state noise, the N value was selected to keep it as small as possible on premise of ensuring the stability of adaptation, so as to improve the adaptation speed. According to the extraction effects from stationary random system state noise with different N values, $N = 6$ is recommended on ABR signal extractions.

Similarly, the adaption of Q_k parameter is achieved by calculating the state noise covariance matrix increment ΔQ_k estimated from ABR state vector estimation error $\bar{\omega}_k$ according (14)–(16), and then the current adaptive Q_k is update by (17) as follows:

$$\bar{\omega}_k = \hat{x}_k - \bar{x}_k \tag{14}$$

$$\hat{\omega}_k = \frac{N-1}{N}\hat{\omega}_{k-1} + \frac{1}{N}\bar{\omega}_k \tag{15}$$

$$\Delta Q_k = \frac{1}{N-1}\left(\hat{\omega}_k - \bar{\omega}_k\right)\left(\hat{\omega}_k - \bar{\omega}_k\right)^T + \frac{1}{N}\left(P_k - AP_{k-1}A^T\right) \tag{16}$$

$$Q_k = \left|diag\left(\frac{N-1}{N}Q_{k-1} + \Delta Q_k\right)\right| \tag{17}$$

According to the above-mentioned model details, the overall procedure of the proposed AKF method is summarized and illustrated in the flowchart of Fig. 1. The ABR recordings in response to repetitive acoustic stimulation were processed by the

AKF algorithm, and the performance was compared with other methods including the time domain averaging and traditional KF in this study.

B. Data Acquisition

Sixteen subjects between the age of 22 and 28 years were recruited for the ABR data acquisition experiments. All the subjects had normal hearing, and no history of neurological diseases were reported. The audiograms of the recruited subjects were less than 20 dB HL across frequencies from 250 to 8000 Hz. The research protocol was approved by the Institutional Review Board of Shenzhen Institutes of Advanced Technology, Chinese Academy of Sciences (IRB Number: SIAT-IRB-190615-H0352). Prior to the experiments, all the subjects gave their written informed consent and provided permission for the publication of their data for scientific purposes.

The ABR signals were acquired by using a 128-channel Neuroscan EEG data acquisition system in an electrically shielded and soundproof booth. For each subject, three gold-plated disc electrodes were used: one was placed on the forehead as the recording electrode, and the other two were placed on the left and right earlobes as the reference and ground electrodes, respectively. Prior to the electrode placement, the skin of the corresponding area was cleaned with an alcohol wipe and was then scrubbed with an abrasive gel to remove oil and sweat that could easily deteriorate the signal quality. Then the subject was seated in a comfortable chair and was encouraged stay as relaxed as possible throughout the experiment. An earphone that was connected to the stimulation generator of the Neuroscan system was inserted into the left ear canal to receive acoustic stimulation. With the subjects kept still throughout the session, the noise-free ABR response signal was simultaneously recorded when the acoustic stimulation was played. The stimulus onset was synchronized to the signal acquisition system through a GPIO trigger interface. Then transient click stimuli with the intensity of 70 dB SPL and a duration of 100 microseconds were presented at a fixed rate of 20 Hz. The stimulus was repeated for a total of 3000 trials, and the response was recorded with a sampling frequency of 20000 Hz.

Moreover, different noises that were commonly observed during practical ABR signal recordings were also collected and the noises were used to mix with the previously recorded noise-free ABR signals to evaluate the performance of different signal extraction strategies. The reason that the ABR and EMG noises were acquired separately was that the target reference (an approximation of the actual ABR signal) could be obtained from the noise-free recordings so that the performance of different extraction methods could be evaluated by the comparison with the target reference. During the noise-recording session, EMG noises were separately measured under three different conditions ('gum chewing', 'mouth opening', and 'milk drinking'). For each condition, the subjects were asked to make the corresponding activity at an interval of 1 second as instructed by the experimenter, and the EMG signals were recorded at the same sample frequency as the ABR session. No acoustic stimulation was provided during this session so that only EMG noises were recorded. Then the EMG noises were added to the original ABR signals with different weights to be as the input of different ABR extraction strategies, so that the performance of different strategies could be tested under different signal-to-noise ratios (SNRs) defined by the following equation:

$$SNR = 20 * \log_{10}\left(\sqrt{\frac{\frac{1}{m}\sum_{i=1}^{m} S(i)^2}{\frac{1}{n}\sum_{j=1}^{n} N(j)^2}}\right) \tag{18}$$

where *S* and *N* stand for the point series of the EEG signal and the EMG noise, respectively, with *m* and *n* referring to the total points number of the data.

C. Signal Processing

In the preprocessing of the original or mixed signals, the recorded data was passed through a software band-pass filter with a cutoff frequency from 100 to 3000 Hz that is commonly used for ABR bandpass filtering. Then the preprocessed signals were segmented according to the onset time stamp trigger of the acoustic stimuli. Thereafter, the segmented waveforms were fed to three different extraction methods: time-domain averaging (TDA), Kalman filter (KF), and adaptive Kalman filter (AKF). For the TDA method, the segmented waveforms of different stimulus presentations were averaged according to the stimulus onsets, and the time waveform 10 ms after the onset was treated as the extracted ABR signal. For the other two methods, the waveform of each segment was processed by the KF and AKF algorithms, respectively, and different segments were fed to the algorithms in the same sequence as the stimulus presentation.

The filter parameters (the noise covariance matrix Q_0 and R_0) needs to be set manually to implement the KF. In practical applications, it is difficult to obtain the optimal values for these filter parameters due to a lack of accurate estimates of real-time noises. Therefore, the filter parameters were set empirically together with a trial and error manner in this study: the values of Q_0 and R_0 were constantly tried and adjusted until the KF was convergent and the extracted ABR signal closely matched the target ABR reference *REF*, which was obtained by averaging the responses of all the 3000 stimulus trials under the noise-free recording condition. For evaluating the performance of different extraction methods, the absolute error (AE, the amplitude difference between the extracted and target ABR waveforms) and the correlation coefficient (CC, the similarity between the extracted and target ABR morphologies) would be calculated as the measures according to the following formula:

$$AE = \frac{1}{L}\sum_{i=1}^{L} |ABR(i) - REF(i)| \tag{19}$$

$$CC = \frac{\sum_{i=1}^{L}\left(ABR(i) - \overline{ABR}\right)\left(REF(i) - \overline{REF}\right)}{\sqrt{\sum_{i=1}^{L}\left(ABR(i) - \overline{ABR}\right)^2 \sum_{i=1}^{L}\left(REF(i) - \overline{REF}\right)^2}} \tag{20}$$

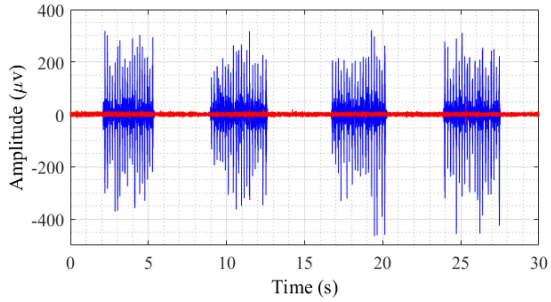

Fig. 2. A typical comparison of the temporal waveform (after preprocessing) of the noise-free ABR (red) and ABR signal mixed with chewing EMG noise (blue).

Where ABR and REF stand for the point series of the extracted and the target ABR waveforms, respectively, with L referring to the total points number of either waveform and i as the i^{th} point; $\overline{ABR}$ and $\overline{REF}$ were the mean values of the point series of the ABR and REF signals, separately. The AE and CC indices were computed under different noise conditions for the three involved methods of TDA, KF and AKF, and their performance in extracting ABR signals was compared thoroughly in different scenarios.

III. Results

A. Comparison of ABR Waveform Morphology

Since the amplitude of ABR signals are usually smaller than 1 μV, other electric physiological signals such as EMG could become strong interference to the ABR recording. Fig. 2 showed a typical comparison of the temporal waveform of the noise-free ABR (red) and ABR signal mixed with chewing EMG noise (blue) recorded in this study. It could be observed that the amplitude of the EMG noise was hundreds of times larger than the ARB signal and therefore it could easily deteriorate the ABR signal quality.

Fig. 3 showed the performance comparison of three different methods (TDA, KF, and AKF) in terms of ABR time waveforms extracted from the noise-free recording (a) and the same recording mixed with chewing EMG noises (b), respectively. As a comparison, the target reference signal (black, REF) extracted from the noise-free recording by 3000 times of averaging was also plotted as a representation of real ABR signal. It could be observed that the ABR waveforms extracted from the noise-free recordings by different methods were entirely overlapped with the target reference signal, as shown in Fig. 3(a). In contrast, the ABR waveforms extracted from the recording mixed with EMG noises showed substantial differences for the three different extraction methods, as illustrated in Fig. 3(b). It could be seen from Fig. 3(b) that the ABR morphology extracted by the AKF method (red) shows the least deviation from the target reference ABR signal (black). The amplitude and latencies of wave I to V matched well between the AKF method and the target reference. However, when it comes to the waveforms extracted by KF and TDA methods (represented by green and blue lines, respectively), it could be observed that the ABR morphologies showed dramatic deviations from the reference

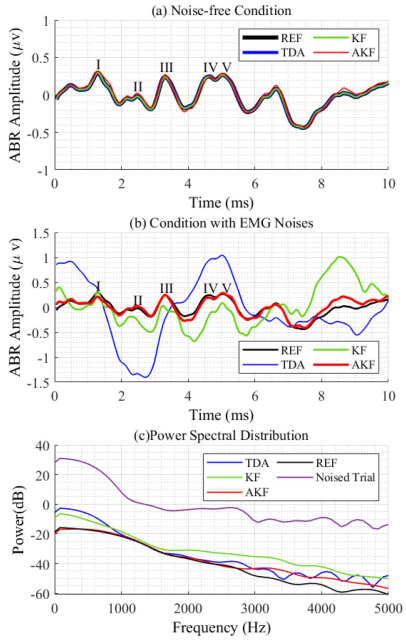

Fig. 3. Comparison of ABR time waveforms for three different methods (TDA, KF, and AKF) extracted from the noise-free recording (a) and the same recording mixed with chewing EMG noises (b), respectively. (c) The power spectral distribution of one noised trial and the extracted ABRs by the three methods. The target ABR (black) obtained from the noise-free recording was plotted as a representation of the target ABR signal.

signal. For the KF method, it could roughly capture the partial trend of the reference ABR signal with a much larger amplitude deviation than the AKF method. Meanwhile, the TDA showed the poorest performance with the worst consistency with the reference signal. The TDA method failed to catch all the wave peaks from I to III, and wave V showed an amplitude above 1 μV, whereas the actual wave V was only around 0.3 μV. To further investigate the performance in the frequency domain, the power spectral distribution of one noised trial and the extracted ABRs by the three different methods were plotted in Fig. 3(c). It could be observed that the power of the noised trial was much higher than those of all the extracted ABRs within the whole frequency band range (from 100 to 3000 Hz). It was also observed that the spectral characteristics of the ABR extracted by the AKF method were closest to that of the referenced clean ABR. The AKF method demonstrated the best performance in inhibiting the spectral contents of both the EMG noises (below 1 kHz) and other high-frequency noises.

B. Effects of Initial Values of Noise Covariance Matrices

With the initial values of the noise covariance matrix Q_0 and R_0 plays an important role in the performance of conventional KF. In this study, the corresponding Q_0 and R_0 parameters were changed independently throughout all possible ranges from 10^{-20} to 10^{20}, with the exponent grows in step one by one. And the AE and CC measures between the extracted ABR and target ABR waveforms for each (Q_0, R_0) combination were computed, with the 3D surface functions shown in Fig. 4. For both the noise-free recording condition in Fig. 4(a) and the cases with

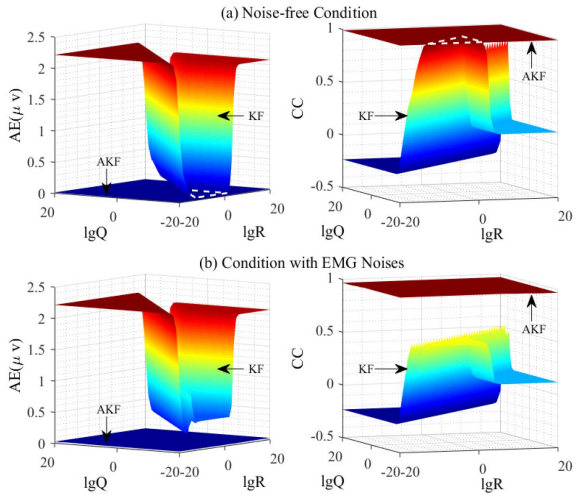

Fig. 4. The AE and CC obtained by AKF and KF methods following the change of the initial values of the noise covariance matrix Q_0 and R_0. (a) The results when the ABR signals were extracted from clean EEG segments. (b) The results when the ABR signals were extracted from EEG segments were interfered with by EMG noise.

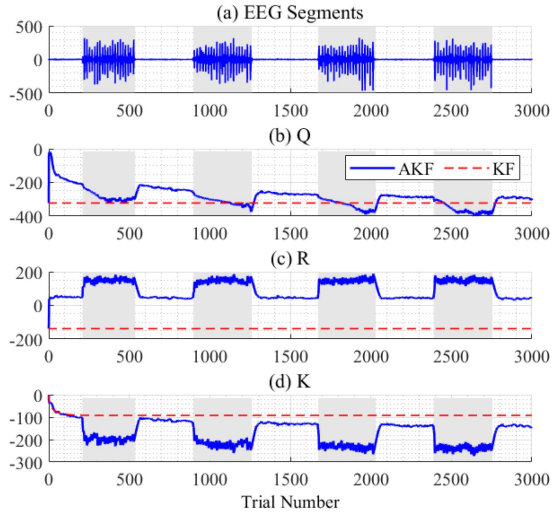

Fig. 5. The trends of estimated noise covariance matrices and the Kalman gain in KF method and AKF method under the effect of EMG noise. (a) Noised EEG signal segments. (b) State noise covariance Q. (c) Measurement noise covariance R. (d) Kalman gain K.

large EMG noises in Fig. 4(b), the AE (indicating the amplitude difference between the extracted and target ABR) could get very close to 0, and the CC (representing the similarity between the extracted and target ABR waveform morphologies) could achieve nearly 1.0 for the proposed AKF, regardless of the initial choice of (Q_0, R_0). It showed that the AKF method could always adaptively change the filter parameters according to the noise conditions so that the extracted ABR signals were quite similar to the target ABR (with small AE and large CC values). In contrast, the performance of the conventional KF was largely dependent on the initial choice of Q_0 and R_0. For noise-free conditions in Fig. 4(a), the KF could achieve performance comparable to the AKF method within a rather narrow range, as shown in white dotted areas of Fig. 4(a). With other inappropriate choices of (Q_0, R_0), the extracted ABR of the KF showed large deviations from the desired target ABR. For recordings with large EMG noises in Fig. 4(b), the performance of the KF was even worse, and it never reaches desired results close to the target ABR regardless of the (Q_0, R_0) choice, suggesting that any fixed-parameter algorithm like the conventional KF could never achieve similar performance compared to the proposed AKF method with adaptive filter parameter adjustment.

As a description of the effect of state and measurement noise covariance in the ABR extraction process, Fig. 5 shows the trends of estimated state noise covariance matrix Q, measurement noise covariance matrix R, and the Kalman gain K in the process of ABR signal extraction from noised EEG segments when using traditional KF method and the proposed AKF-based technique, respectively. As shown in Fig. 5(a), in a piece of click stimulation-induced EEG segments from which ABR would be extracted, EMG noise that is several times of the EEG amplitude was mixed in gray shaded segments. Fig. 5(b) and (c) show the change of the noise covariance matrix Q and R with the increase of trial number. Here the Q and R matrixes are represented by the ratio of the matrix trace to the matrix dimension. It can be found that for the traditional KF method, the Q and R matrixes keep the initial value unchanged throughout the process. While for AKF method, the Q and R matrixes were adjusted dynamically. Corresponding to the appearance of noise in each time, a dynamic fluctuation will appear in the Q and R curve with Q gradually decreases, and R quickly increases to a stable fluctuation range, respectively. Conversely, when the noise disappears, the Q and R curves will oscillate back to another stable fluctuation range. By adding different types and different amplitudes of random noises to the ABR signals, it was observed that the adjustment of R and Q in the AKF method could consistently follow the rapid change in noise characteristics. Moreover, the amplitude of the parameter adjustment seemed to be in proportion with the noise magnitude. When it comes to the curve of Kalman gain K in Fig. 5(d), which defines the updating weight of each innovation information, it can be found that the K curve for KF method drops rapidly in the initial stage and just keep it after reaching a certain range. For the AKF method, before the noise appears, the curve maintained a monotonous downward trend, indicating that as the number of repetitions increases, the useful information that can be extracted from the new epoch gradually decreases, but it still exists. However, when the noise appears, the K curve drops quickly, indicating that the new information provided by the noised epochs to the final result curve is almost none, thus achieving the purpose of suppressing the interference of the noise on the result curve. Here, logarithmic display is used for the Q, R and K curve.

C. Effects of Stimulus Trial Number

The stimulus trial number required to obtain a satisfactory ABR waveform is another important factor that affects the real-time application of the clinical ABR measurements. When the trial number is adequate, the extracted ABR waveform

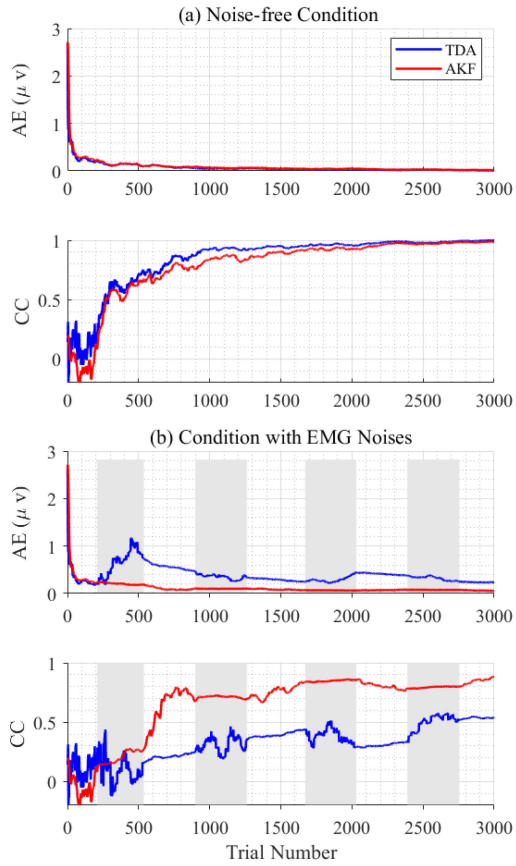

Fig. 6. The trends of AE and CC between the reference ABR signal and the extracted ABR waveform as functions of stimulus trial number, when the ABR recording was noise-free (a) and mixed with EMG noises (b).

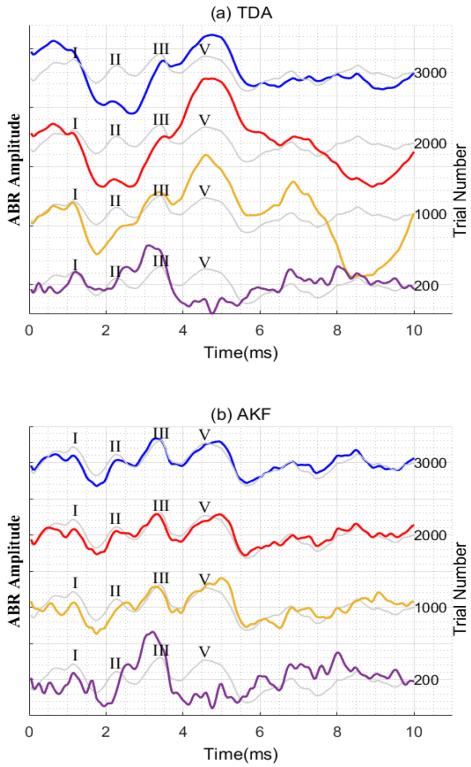

Fig. 7. The ABR waveforms were extracted by the TDA and the AKF method for different trial numbers when the ABR recording was mixed with EMG noises. The grey lines for each trial number represent the reference ABR waveform obtained by averaging the responses of all the 3000 noise-free trials.

morphology will be quite close to the reference ABR signal, indicated by small values of absolute error (AE) and large values of correlation coefficient (CC). Fig. 6 shows the trends of AE and CC between the reference ABR signal and the ABR waveform extracted by TDA and AKF methods when the stimulus trial number gradually increased. It could be seen from Fig. 6(a) that, when the ABR recording was noise-free, the AE curves of both methods declined with the increase in the trial number, and they almost overlapped with each other over the entire range. It showed the largest decline rate when the trial number increased from 0 to around 1000, and no significant reduction was observed when the repetition further increased. The absolute error fell below 0.1 μV when the repetition was 1000. The CC curves (bottom panel, Fig. 6(a)) showed consistent findings for the noise-free case: the correlation coefficient dramatically increased from 0 with the initial increase in the trial number and then became saturated when it further increased from about 1000. However, when the ABR recordings were mixed with large EMG noises (occured within shadowed areas), substantial differences were found in the AE and CC curves between the TDA and AKF methods. As could be observed from the top panel in Fig. 6(b), the introduction of the first EMG noise (trial number from 250 to around 500) caused the AE of the TDA method to increase greatly. In contrast, the AE curve of the AKF method did not seem to be much affected by the EMG noise, and the AE values decreased monotonously as the trial number increased, similar to the noise-free case. The AE value of the AKF method was always smaller than that of the TDA method at the same trial number. For the CC curves when EMG noises were added (bottom panel, Fig. 6(b)), the CC curve of the TDA method deteriorated every time when the EMG noises were added, and the correlation values remained at rather low levels as a result, with a CC value of only 0.5 when the trial number reached a maximum of 3000. The negative impacts of the EMG noises on the CC curve seemed much smaller for the AKF method. As the trial number increased, the introduction of the EMG noise only resulted in the slow-down of the CC increase speed but did not cause a reduction of CC values observed in the case of the TDA method. The smaller AE values and larger CC values in Fig. 6(b) indicated that the AKF method could obtain better ABR morphologies when large EMG noises were introduced.

Fig. 7 showed the ABR waveforms extracted by the TDA and the AKF methods for different stimulus trial numbers when the ABR recording was mixed with EMG noises. The ABR waveforms (gray lines) obtained by averaging the responses of all the 3000 noise-free trials were also plotted as a reference. As observed from the figure, when there were only 200 stimulus repetitions, the waveforms extracted by the two methods both showed large deviations from the reference ABR signal. When

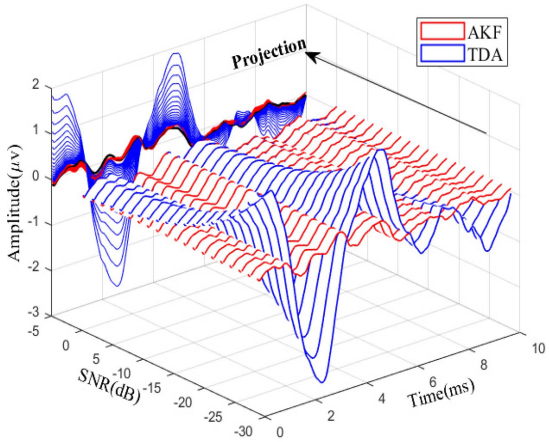

Fig. 8. The ABR waveforms extracted from recordings mixed with different levels of gum chewing EMG noises.

the number of repetitions increased to 1000, the waveform extracted by the AKF method succeeded in catching all peaks from wave I to wave V with some amplitude and latency deviations. However, the waveform extracted by the TDA method failed to catch accurate peak components and showed large amplitude discrepancies due to the influence of EMG noise. With the repetition number increased to 2000 and 3000, the difference between the extracted waveform by AKF and the reference ABR further decreased, and the signal quality of the AKF method showed a close match to the reference ABR. However, for the TDA method, the deviation between the extracted waveform and the reference ABR still remains at high levels due to the influence of the EMG noises. The ABR waveform morphology was still not reliable even when the trial number reached the maximum.

D. Performance Under Different Noise Conditions

In this study, the performance of the proposed AKF method under different noise conditions was also investigated. The gum-chewing EMG noises were multiplied by different scales and then added to the noise-free ABR recording to achieve a signal-noise ratio (SNR) from 5 to −30 dB. Then the ABR signal was extracted from these noised signals by TDA and AKF method, respectively, with the ABR waveforms extracted under different noise levels displayed in Fig. 8. The curves corresponding to different noise levels were illustrated in a 3D form, so that it would be easier to compare the differences. To facilitate the observation, the projections of these waveforms on the same plane together with the referenced ABR signal represented by the black line were also plotted together. It could be found that the ABR waveforms of the TDA method (represented by blue lines) showed dramatically increasing deviations from the reference as the noise level increased. The wave V amplitude could be as large as about 2 uV, which was 10 times larger than the reference ABR signal. On the contrary, the waveforms extracted by the AKF method (represented by the red lines) showed much smaller deviations from the reference ABR, and the noise level seemed to have little effect on the AKF performance. Even when the SNR was as low as −30 dB, the extracted ABR of the AKF method demonstrated rather a close match with the target ABR reference.

TABLE I
PARAMETERS FOR TWO METHODS UNDER DIFFERENT NOISE LEVEL

SNR (dB)		0	-20	-40	-60	-80
Method: TDA	AE (μV)	0.037	0.369	3.693	36.93	369.3
	CC	0.957	0.414	0.167	0.139	0.137
Method: AKF	AE (μV)	0.031	0.060	0.069	0.077	0.092
	CC	0.968	0.868	0.839	0.810	0.756

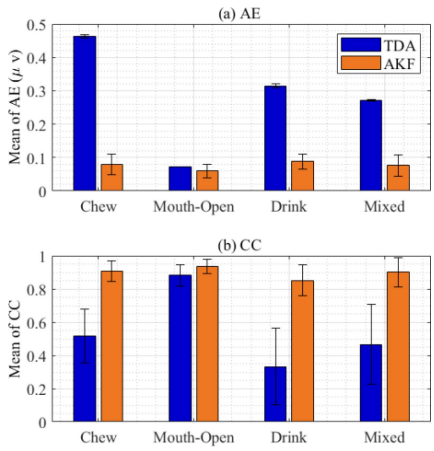

Fig. 9. Comparison of the mean and standard deviation of the CC and AE between the extracted ABR and the target reference for the TDA and AKF methods under four different types of noise conditions.

The AE and CC between the extracted waveforms and the referenced ABR were calculated under different noise levels and the numeral comparison was listed in Table I. It could be observed that when the SNR decreased from 0 dB to −80 dB, the AE of the TDA method increased from 0.037 μV to 369.3 μV, and the CC decreased from 0.957 to 0.137 monotonously. However, the AE of the AKF changed from 0.031 μV to 0.092 μV when the SNR was from 0 to −80 dB. The AE remained rather small and stable across a wide range of SNR. Meanwhile, the CC results of the AKF method also showed a much smaller decrease when the noise level increased.

Moreover, the influence of different types of noises on the performance of different extraction methods was also investigated. Four different types of noises were investigated: 'gum chewing', 'mouth opening', 'milk drinking' and mixed noise by adding all above noises. The statistics of the AE and CC values between the extract signals and the target reference were calculated for all the 16 subjects and the results were shown in Fig. 9. It could be observed the AE values of the AKF method were as low as below 0.1 μV across all different noise types, while the AE values of the TDA method were much higher, with the AE more than five times larger than the AKF method under the gum-chewing condition. On the other hand, the CC values between the extracted ABR signal and the target reference were above 0.85 for the AKF method under all different noise conditions, also significantly higher than those of the TDA method.

IV. Discussion

Given the close relation of the ABR signal with the functioning status of the auditory pathway, the ABR waveform morphology is rather important for the clinical diagnoses of various auditory neuropathies [2]–[7]. However, the ABR signal has a small amplitude as low as 0.1 μV, making it quite challenging to measure such a weak signal with satisfactory qualities. The ABR signal recordings are often contaminated by various noises with several orders of larger magnitude, such as ECG introduced by the heart beats, and EMG caused by crying and drinking, especially for children [12], [13]. The introduction of large-amplitude noises increases the difficulty of ABR signal extraction. Time-domain averaging (TDA) technique has been frequently used to suppress the background noise and realize the ABR signal enhancement in both the clinic and scientific research [2], [9]–[11], [37]. However, the TDA method usually requires large trial number (up to 3000) of stimulus repetition, leading to too long testing time. Some existing solutions such as artifact rejection and weighted average require the prior knowledge of noise for parameter setting, which is highly dependent on the experience of the tester and increases the difficulty in practical applications [11], [24], [25].

In this study, a new ABR extraction method based on AKF was proposed to improve the ABR signal quality in noisy recording environments. By introducing adaptive updating rules, the proposed AKF method can dynamically track the real-time changes of various noises to improve the performance of the conventional KF. In technical details, the AKF-based method uses the innovation information and state vector estimation error to adaptively estimate the state and measurement noise covariance matrices Q_k and R_k for each iteration. The proposed method reduces the impact of noises by controlling of the contribution of each trial response according to the instantaneous change of the noise covariance.

A. Effects of Adaptive Adjustment of Noise Parameters

Although the effectiveness of using the KF algorithm for ABR extraction has been demonstrated in previous studies [24], [25], the requirement of manually setting the filter parameters (the state and measurement noise covariance matrices, Q_0 and R_0) make it difficult to use in practical applications. The manual choice of filter parameters is highly dependent on the users' experience, and undesired filter divergence will occur due to improper settings of filter parameters [28]. Moreover, the conventional KF with fixed parameter settings is not suitable for the circumstances with time-varying noise sources. The proposed AKF-based ABR extraction method overcomes the problem by dynamically estimating Q and R values using the innovation and state vector estimation error according to instantaneous noise conditions (12)–(17). Fig. 5 showed that the estimation of Q and R could adaptively track the variation of noise levels so that the AKF method could dynamically change the Kalman gain *K* to reduce the contributions of the current measurement if it contained too much noise. In this way, the initial value Q_0 and R_0 has little effect on the performance of the proposed AKF-based ABR extraction method, demonstrated by its capacity of adaptively adjusting to the optimal filter parameters in response to all different initial Q_0 and R_0 values, as shown in Fig. 4. Due to its automatic adaptation of filter parameters, the proposed AKF-based method showed great performance by the close matching with the ABR target when the recording contained large chewing EMG noises (Fig. 3). In contrast, the conventional KF with fixed parameter settings demonstrated much poorer performance with a much larger deviation from the ABR target. The TDA method commonly used in the clinic showed the largest ABR contamination by the EMG noise, leading to unusable test results under such noise conditions (Fig. 3). The superior performance of the AKF method was also confirmed by the smaller absolute error (AE) and larger correlation coefficient (CC) between the extracted and target ABR signals, as shown in Fig. 6. There are different types of methods to adjust the knowledge about current noise and adapt the filter parameters accordingly, including the Bayesian, maximum likelihood and correlation (autocorrelation) methods [29], [33]. The proposed AKF meothod in this study employed the idea of covariance matching that was originally developed for estimating linear or nonlinear variable of interest. The concept of recursive estimation (12)–(17) is adopted during the covariance matching process of the AKF method so that small computation load and fast convergence could be achieved, making it rather suitable for real-time scenarios with fast-response requirement and embedded applications with limited processing power.

B. Impacts on Required Trial Number

Since the ABR has a rather low amplitude, large trial numbers of stimulus repetition are commonly required to obtain satisfactory ABR waveform morphologies, especially when the subject is difficult to keep quiet. However, a large trial number usually means rather long testing time, which is another problem that worth to pay attention in practical applications [2]. The signal-to-noise ratio (SNR) of the extracted ABR signal in time domain averaging (TDA) technique commonly used in the clinic increases by a factor equal to the square root of the trial number and therefore the large trial number is preferred by the TDA method [9]–[11]. As observed in Fig. 6(a), the absolute error (AE) in the noise-free condition showed a rapid initial decrease and then approached nearly 0 after about 1000 trials for the TDA method, which is consistent with the findings in previous studies [2], [37]. However, the performance of the TDA can be easily affected by the involvement of large-amplitude noises, and even longer testing time is required to cancel the large noise impacts. It can be confirmed by the observation of Fig. 6(b) in which the ABR recording was seriously contaminated by large EMG noises. Because of the large noises, the AE of the TDA method still remained at very high levels even when the trial number reached the maximum. It suggested that more than 3000 trials were needed to obtain a desired ABR signal (Fig. 6(b)), leading to the burden increase of data collection and further extension of testing time. In this regard, corresponding solutions such as artifact rejection and weighted average are employed to improve the robustness of ABR extractions [13].

However, for these solutions, it is not easy to choose the optimal artifact rejection criteria, and the weight coefficients is largely dependent on the accurate estimate of the noise level, especially when the noises are nonstationary. To better solve this problem, the method of AKF proposed in this study aims to inhibit the noise interferences and therefore reduce the required trial number of stimulus repetition, as well as the testing time. As shown in Fig. 6(b), the absolute error between the ABR signal extracted by the AKF method and the target ABR seemed to have little disturbance by the introduction of large EMG noises. The correlation coefficient of the AKF method was also much higher when compared with the TDA method. The comparison in Fig. 7 also demonstrated that the AKF method could achieve satisfactory ABR morphologies much earlier than the TDA method when extracting ABR signals from noisy recordings, with much less required trail number of stimulus repetitions. The superior performance of the proposed AKF method is mainly attributed to its capacity of adaptive adjustment of the filter parameters, so that the instantaneous noise burst could be identified promptly, and the contribution of the noise-containing recording could be turned down accordingly. It should also be noted that the performance of the AKF method is almost not deteriorated by the increase in noise amplitude (Fig. 8), making it a great candidate for quick measurements of ABR signals in environments with large instant noises or interferences.

C. Robustness to Different Noise Types and Levels

Different types and levels of noises are usually inevitably mixed with the target ABR signals in clinical or laboratory recordings, and therefore the robustness of the ABR extraction algorithm to different noise types and levels is also an important factor to concern in practical applications. The noises embedded in the recordings are usually several orders larger than the ABR signal (Figs. 2 and 5(a)), and cause large negative impacts on the performance of the conventional TDA and KF methods (Figs. 3(b) and 6), with the extracted waveforms having different degrees of deviation from the target ABR signal even after 3000 trials of stimulus repetition (Fig. 3(b)). Without careful handle of the embedded noises, the clinical diagnostic accuracies that largely rely on the extracted ABR waveform morphologies will be negatively affected as a consequence. In this study, the AKF method was proposed to prevent different noises from deteriorating the ABR signal quality, so that more reliable ABR morphologies could be obtained within a short period of time. As observed in Fig. 8, the extracted ABR waveform by the AKF method always closely matched the ABR target when the noise level kept increasing, and there was small decrease in the extracted ABR quality even when the signal to noise ratio (SNR) was as low as -30 dB (Fig. 8). When the SNR further decreased to as low as -80 dB (Table I), the absolute error was only 0.092, and the correlation coefficient could remain above 0.75 for the AKF method, indicating that the AKF method still has relatively good performance when the noise was 10^4 times larger than the ABR signal. In contrast, the performance of the conventional TDA method is rather sensitive to the noise level, and the extracted ABR is almost not usable when the SNR is only -20 dB, as shown in Fig. 8 and Table I. In this study, EMG noises of different types (gum chewing, mouth opening, milk-drinking or a mixture of them) were also measured, and then mixed with the clean ABR recording to evaluate the performance of the proposed AKF method. Fig. 9 illustrated that, for all different noise types, the AKF method showed consistently great performance, with much smaller absolute errors and much higher correlation coefficients when compared with the TDA method. These results indicate that the proposed AKF method could significantly increase the robustness to different noise types and levels. The robustness is achieved by adaptively adjusting the weight according to the noise characteristics of the current measurement, so as to inhibit the negative impacts of large amplitude noises.

Although the proposed AKF method could reduce the contribution of the noised trials on the extraction result, it should still be noted that trials with maximum amplitudes greater than 20 μV are usually deemed to have too much noise and should be better rejected instead of processed with any method including the proposed AKF [4], [12], [17], [38]. Another point should be noted is that the AKF demonstrated significant superiority to suppress the impacts of transient noises instead of constant noises. When certain noises were constantly present throughout the whole recording process (such as the power-line noise interference), pre-processing techniques such as notch filter should be considered before the AKF method is employed for ABR extraction. It is also worth mentioning that the proposed AKF method is not restricted only to the application of ABR extraction. In fact, it is applicable to the extraction of all evoked potentials with repetitive stimulus and embedded noises, such as visual evoked potential, somatosensory evoked potential, and motor evoked potential.

V. Conclusion

The ABR signals are weak electrical voltages originating from the stations of the auditory pathway, and various sources from the environment can cause significant interferences to the ABR recordings. To extract low-amplitude ABR signal from large environmental noises, a robust extraction approach based on adaptive Kalman filter (AKF) was proposed, and its performance was thoroughly investigated in this study. The results of this study indicated that the proposed AKF-based method can dynamically estimate and adjust the noise covariance matrix of the traditional Kalman filter (KF), and therefore the impacts from strong transient interferences could be extensively minimized. And the proposed AKF method could obtain the best ABR waveform morphologies in the presence of EMG and EEG noises in comparison to traditional methods of time-domain averaging (TDA) or KF. The problem of inaccurate ABR extraction caused by improper parameter settings in traditional KF could be avoided by dynamic estimation of the noise covariance matrices Q and R, regardless of the initial choice of these matrices. Compared with the time domain average method in which the impacts of the large-amplitude interference could be long lasting, the AKF method could minimize such interferences by assigning smaller weights to the corresponding repetition. Finally, the results showed that the proposed AKF method could extract

satisfactory ABR signal waveforms under different noise types and signal-to-noise ratios from −80 to 0 dB. The AKF method of this study could be a great candidate to improve the signal quality and increase the robustness of current ABR measurements. It acts like an automatic artifact rejection helping shielding the impact of transient noises. If the noises or interferences outside shielding room persist for a long time during data collection, besides the AFK method, other specific filtering techniques would be needed to reduce the effects of the persisted noises for ABR extraction. The proposed AKF method could also be useful for the extraction of other evoked potentials in the presence of various environmental noises and interferences.

REFERENCES

[1] C. Escera and N. Gorina-Careta, "Auditory brainstem responses," *Encyclopedia Comput. Neurosci.*, vol. 423, no. 2, pp. 1–4, 2019.

[2] Y. Sokolov *et al.*, *Integrity Technology: Enabling Practical ABR*. Toronto, ON, Canada: Vivosonic, Inc., 2006, pp. 1–12.

[3] K. Krumbholz *et al.*, "Automated extraction of auditory brainstem response latencies and amplitudes by means of non-linear curve registration," *Comput. Methods Programs Biomed.*, vol. 196, 2020, Art. no. 105595.

[4] L. W. Norrix *et al.*, "Clinicians' guide to obtaining a valid auditory brainstem response to determine hearing status: Signal, noise, and cross-checks," *Amer. J. Audiology*, vol. 27, no. 1, pp. 25–36, 2018.

[5] X. Li and Q. Wang, *Fundamental and Application of Auditory Evoked Response*, Beijing, China: Peoples Mil. Med. Press, 2015.

[6] F. Michel and K. F. J. Rgensen, "Comparison of threshold estimation in infants with hearing loss or normal hearing using auditory steady-state response evoked by narrow band CE-chirps and auditory brainstem response evoked by tone pips," *Int. J. Audiology*, vol. 56, no. 2, pp. 99–105, 2017.

[7] R. Feirn *et al.*, "Guidelines for the early audiological assessment and management of babies referred from the newborn hearing screening programme," Early Assessment Guidelines Version 6, British Society of Audiology, U.K., Oct. 2013.

[8] T. Pander, "A new approach to robust, weighted signal averaging," *Biocybernetics Biomed. Eng.*, vol. 35, no. 4, pp. 317–327, 2015.

[9] J. T. Sanchez and D. Gans, "Effects of artifact rejection and Bayesian weighting on the auditory brainstem response during quiet and active behavioral conditions," *Amer. J. Audiol.*, vol. 15, no. 2, pp. 154–163, Dec. 2006.

[10] F. H. Y. Chan *et al.*, "Detection of brainstem auditory evoked potential by adaptive filtering," *Med. Biol. Eng. Comput.*, vol. 33, no. 1, pp. 69–75, 1995.

[11] M. Don and C. Elberling, "Evaluating residual background noise in human auditory brain-stem responses," *J. Acoustical Soc. Amer.*, vol. 96, no. 5, pp. 2746–2757, 1994.

[12] B. Cone and L. W. Norrix, "Measuring the advantage of Kalman-weighted averaging for auditory brainstem response hearing evaluation in infants," *Amer. J. Audiology*, vol. 24, no. 2, pp. 153–168, 2015.

[13] A. Marcoux and I. Kurtz, "Noise reduction to achieve quality ABR measurement," *Can. Hear. Rep.*, vol. 8, no. 3, pp. 19–23, 2012.

[14] N. Ikawa, A. Morimoto, and R. Ashino, "A new detection method for short latency of auditory evoked potentials using stationary wavelets," in *Proc. Int. Conf. Wavelet Anal. Pattern Recognit.*, Chengdu, China, 2018, pp. 82–88.

[15] A. C. De Silva and M. A. Schier, "Evaluation of wavelet techniques in rapid extraction of ABR variations from underlying EEG," *Physiol. Meas.*, vol. 32, pp. 1747–1761, 2011.

[16] I. Kurtz *et al.*, "Kalman filtering in recording auditory evoked potentials," in *Proc. 28th Midwinter Meeting Assoc. Res. Otolaryngol.*, New Orleans, LA, USA, 2005, pp. 19–24.

[17] L. W. Norrix *et al.*, "The effect of Kalman-weighted averaging and artifact rejection on residual noise during auditory brainstem response testing," *Amer. J. Audiology*, vol. 28, no. 1, pp. 114–124, 2019.

[18] M. S. John *et al.*, "Weighted averaging of steady-state responses," *Clin. Neurophysiol.*, vol. 112, no. 3, pp. 555–562, 2001.

[19] S. M. K. Madsen *et al.*, "Accuracy of averaged auditory brainstem response amplitude and latency estimates," *Int. J. Audiology*, vol. 57, no. 5, pp. 345–353, 2018.

[20] I. Kurtz *et al.*, "System and method for adaptive stimulus-response signal filtering," U.S. Patent 8484270, 2013.

[21] C. Elberling and M. Don, "Quality estimation of averaged auditory brainstem responses," *Scand. Audiology*, vol. 13, no. 3, pp. 187–197, 1984.

[22] J. Leski, "New concept of signal averaging in time domain," in *Proc. Annu. Int. Conf. IEEE Eng. Med. Biol. Soc.*, 1991, vol. 13, pp. 367–368.

[23] J. K. Wheeler, "The effect of Kalman weighted filtering and in-situ pre-amplification on the accuracy and efficiency of ABR threshold estimation," Ph.D. Dissertations 42 & Theses - Gradworks, James Madison Univ., Harrisonburg, VA, USA, 2011.

[24] R. Luke and J. Wouters, "Kalman filter based estimation of auditory steady state response parameters," *IEEE Trans. Neural Syst. Rehabil. Eng.*, vol. 25, no. 3, pp. 196–204, Mar. 2017.

[25] S. Aydin, "Comparison of basic linear filters in extracting auditory evoked potentials," *Turkish J. Elect. Eng. Comput. Sci.*, vol. 16, no. 2, pp. 111–123, 2008.

[26] K. Myers and B. Tapley, "Adaptive sequential estimation with unknown noise statistics," *IEEE Trans. Autom. Control*, vol. 21, no. 4, pp. 520–523, Aug. 1976.

[27] R. Mehra, "On the identification of variances and adaptive Kalman filtering," *IEEE Trans. Autom. Control*, vol. 15, no. 2, pp. 175–184, Apr. 1970.

[28] L. Wang and G. Hugues, *System Identification, Environmental Modelling, and Control System Design*. London, U.K.: Springer-Verlag, 2012.

[29] R. Mehra, "Approaches to adaptive filtering," *IEEE Trans. Autom. Control*, vol. 17, no. 5, pp. 693–698, Oct. 1972.

[30] M. S. Mohan *et al.*, "Introduction to the Kalman filter and tuning its statistics for near optimal estimates and Cramer Rao bound," Dept. Elect. Eng., Indian Inst. Technol. Kanpur, *arXiv-1503*. 2015.

[31] I. Hashlamon and K. Erbatur, "An improved real-time adaptive Kalman filter with recursive noise covariance updating rules," *Turkish J. Elect. Eng. Comput. Sci.*, vol. 24, no. 2, pp. 524–540, 2016.

[32] S. Akhlaghi, N. Zhou, and Z. Huang, "Adaptive adjustment of noise covariance in Kalman filter for dynamic state estimation," *IEEE Power Energy Soc. Gen. Meeting*, Jul. 2017, pp. 1–5.

[33] Y. Huang *et al.*, "A novel adaptive Kalman filter with inaccurate process and measurement noise covariance matrices," *IEEE Trans. Autom. Control*, vol. 63, no. 2, pp. 594–601, Feb. 2018.

[34] X. R. Li and Y. Bar-Shalom, "A recursive multiple model approach to noise identification," *IEEE Trans. Aerosp. Electron. Syst.*, vol. 30, no. 3, pp. 671–684, Jul. 1994.

[35] A. H. Mohamed and K. P. Schwarz, "Adaptive Kalman filtering for INS/GPS," *J. Geodesy*, vol. 73, no. 4, pp. 193–203, 1999.

[36] J. Brian *et al.*, "A new autocovariance least-squares method for estimating noise covariances," *Automatica*, vol. 42, no. 2, pp. 303–308, 2006.

[37] H. Wimalarathna *et al.*, "Comparison of machine learning models to classify auditory brainstem responses recorded from children with auditory processing disorder," *Comput. Methods Programs Biomed.*, vol. 200, 2021, Art. no. 105942.

[38] G. Lightfoot and J. Stevens, "Effects of artefact rejection and Bayesian weighted averaging on the efficiency of recording the newborn ABR," *Ear Hear.*, vol. 35, no. 2, pp. 213–220, 2014.